Atomic and Electronic Structures of Fluorinated BN Nanotubes: Computational Study

ARTICLE *in* THE JOURNAL OF PHYSICAL CHEMISTRY B · JANUARY 2007

Impact Factor: 3.3 · DOI: 10.1021/jp063257d · Source: PubMed

4 AUTHORS, INCLUDING:

Zhen Zhou
Nankai University
213 PUBLICATIONS **6,982** CITATIONS
SEE PROFILE

Jijun Zhao
Dalian University of Technology
390 PUBLICATIONS **8,454** CITATIONS
SEE PROFILE

Zhongfang Chen
University of Puerto Rico at Rio Piedras
221 PUBLICATIONS **8,038** CITATIONS
SEE PROFILE

Atomic and Electronic Structures of Fluorinated BN Nanotubes: Computational Study

Zhen Zhou,*,† Jijun Zhao,‡ Zhongfang Chen,*,§ and Paul von Ragué Schleyer§

Institute of New Energy Material Chemistry, Institute of Scientific Computing, Nankai University, Tianjin 300071, People's Republic of China, State Key Laboratory of Materials Modification by Laser, Electron, and Ion Beams and College of Advanced Science and Technology, Dalian University of Technology, Dalian 116023, People's Republic of China, and Department of Chemistry and Center for Computational Chemistry, University of Georgia, Athens, Georgia 30602

Received: May 26, 2006; In Final Form: October 16, 2006

The atomic and electronic structures of fluorinated BN nanotubes (BNNTs) were investigated by generalized gradient approximation (GGA) density functional theory (DFT). The reaction energies of F_2 with pristine single-walled BNNTs to form fluorinated BNNTs are exothermic up to 50% coverage. At lower F coverages (below 50%), fluorines prefer external attachments to boron atoms and stay as far away as possible. At 50% F coverage, fluorines favor attachment to all the boron atoms of the outer surface energetically. Such preferable fluorination patterns and highly exothermic reaction energies hold true for double-walled (and multiwalled) BNNTs when the outer tube surface is considered. Fluorination transforms BNNTs into p-type semiconductors at low F coverages, while high F coverages convert BNNTs into p-type conductors. Therefore, the electronic and transport properties of BNNTs can be engineered by fluorination, and this provides potential applications for fluorinated BNNTs in nanoelectronics.

1. Introduction

Boron nitride nanotubes (BNNTs) have striking structural similarities to their close cousins, the carbon nanotubes (CNTs).[1] However, the large ionicity of the B−N bonds endows BNNTs with many properties that differ from those of their carbon analogues. For example, BNNTs are insulators with a wide band gap (ca. 5 eV) that depends weakly on the diameter, the helicity, and the number of tube walls.[2] The uniformity of electronic properties and the relative chemical inertness of BNNTs are key advantages for their application to nanoelectronics.[3]

Tailoring the electronic properties of BN nanotubes is another promising prospect. To realize this purpose, heteroatom substitution,[4] native defects,[5] endohedral encapsulation of transition metals[6] as well as fullerene,[6b] exohedral coating (by stannic oxide),[7] and exohedral adsorption by first-row[8] and transition metal atoms[9] have been employed. Very recently, BN tube fluorination has been achieved during the process of tube growth by Tang et al.[10] It was found that 5% F doping (involving both substitution and addition) decreases the resistivity of the BNNTs by 3 orders of magnitude and converts the originally insulating BN nanotubes into semiconductors. The effects of F substitution[11a,b] and low ratio adsorption[8,11] on the band structures have been investigated theoretically.

Fluorination is an important reaction for carbon nanotubes[12] since their solubility, conductivity, and chemical reactivity can be modified significantly. Fluorinated single-walled carbon nanotubes (F-SWCNTs) can have very large degrees of functionalization (up to F/C = 0.5) and are much more soluble than pristine tubes.[13] Thus, fluorination serves as a route to carbon nanotubes, amenable to further chemical modifications. Moreover, fluorination can tune the band structures of carbon nanotubes (for example, F-zigzag (18,0) tubes are not metallic[14]).

Similarly, fluorination might increase the solubility of BNNTs,[15] offer intermediates for further chemical modification, and allow the electronic properties of BNNTs to be engineered by controlling the fluorination pattern and ratio. Despite recent experimental and computational investigations,[10,11] many questions are still pending. Are BNNTs more or less reactive toward fluorination than their carbon analogues? What is the highest possible fluorine coverage for F-BNNTs? What is the most favorable addition pattern for F-BNNTs with high modification ratios? How does the fluorination affect the electronic properties of BNNTs? Is it possible to convert BNNTs into conductor forms by fluorination? In this paper, periodic boundary density functional theory (DFT) computations were performed to address these questions.

2. Computational Methods

Our DFT calculations employed the plane-wave pseudopotential technique implemented in the Vienna ab initio simulation package (VASP).[16] The generalized gradient approximation (GGA) with the PW91 functional,[17] and a 360 eV cutoff for the plane-wave basis set were used in all the computations. The electron−ion interactions were modeled by the ultrasoft pseudopotentials. To simulate infinitely long (rather than truncated) nanotube systems, one-dimensional (1-D) periodic boundary condition (PBC) was applied along the tube axis. Interactions between F atoms and their 1-D periodic images were avoided in our computational supercell models, which include two unit cells of the zigzag tube (for example, supercell length $c = 8.64$ Å for (10,0) BN nanotube (Figure 1a)). The positions of all the atoms in the supercell were fully relaxed during the geometry optimizations of the systems studied. Five k points were used for sampling the 1-D Brillouin zone, and the convergence threshold was set as 10^{-4} eV in energy and 10^{-3} eV/Å in force.

* Corresponding authors. E-mail: zhouzhen@nankai.edu.cn (Z.Z.); chen@chem.uga.edu (Z.C.).
† Nankai University.
‡ Dalian University of Technology.
§ University of Georgia.

10.1021/jp063257d CCC: $33.50
Published on Web 12/08/2006

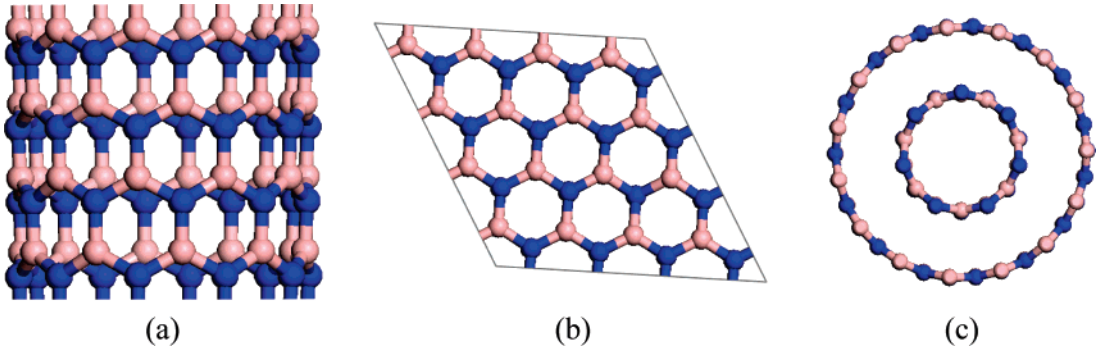

Figure 1. Schematic drawing for different models used in this investigation. (a) (10,0) BN SWNT as an example of a series of zigzag BN tubes (side view); (b) hexagonal BN graphitic sheet; (c) BN (7,0)@(15,0) DWNT (top view). B and N atoms are denoted using orange and blue balls, respectively.

Based on the equilibrium structures, 21 *k* points were then used to obtain band structures.

The nomenclature of BN (*n*,*m*) nanotubes and C (*n*,*m*) nanotubes is similar. As BN nanotubes are known experimentally to adopt zigzag structures,[18] only models for zigzag single-walled nanotubes (SWNTs) were computed from (7,0) to (16,0) with tube diameters between 0.55 and 1.3 nm. For comparison, we studied the hexagonal BN graphitic sheet by employing a 4 × 4 supercell on the graphene plane (Figure 1b). In addition to SWNTs, we also studied double-walled nanotubes (DWNTs). A combination (7,0)@(15,0) DWNT (Figure 1c), which has been calculated to be the smallest possibility among the most stable configurations, was used as the model system.[19]

In order to simulate F-attached (10,0) BN nanotubes with different F coverages, initial computational supercell models including one (c = 4.32 Å), two (c = 8.64 Å), or three unit cells (c = 12.96 Å) were adopted. The unit cell length, c, was also optimized at the 50% F coverage.

The F adsorption energy (E_{ads}) is defined as $E_{ads} = [E_{(BNNT-nF)} - E_{(BNNT)} - (n/2)E_{(F2)}]/n$, where $E_{(BNNT-nF)}$, $E_{(BNNT)}$, and $E_{(F2)}$ stand for the total energies of the F adsorbed nanotube, the nanotube, and the F_2 molecule, respectively, and n stands for the number of the fluorine atoms. The F adsorption energy on SWCNTs is defined similarly. By this definition, $E_{ads} < 0$ corresponds to exothermic adsorption leading to minima stable toward dissociation. Note that the energy of a single F atom, as in ref 9, was not used as reference; instead, half the energy of the F_2 molecule was employed for the adsorption energy calculations in this paper. Such a reference (1/2 F_2) allows evaluating both physisorption and chemisorption energies with a uniform equation.

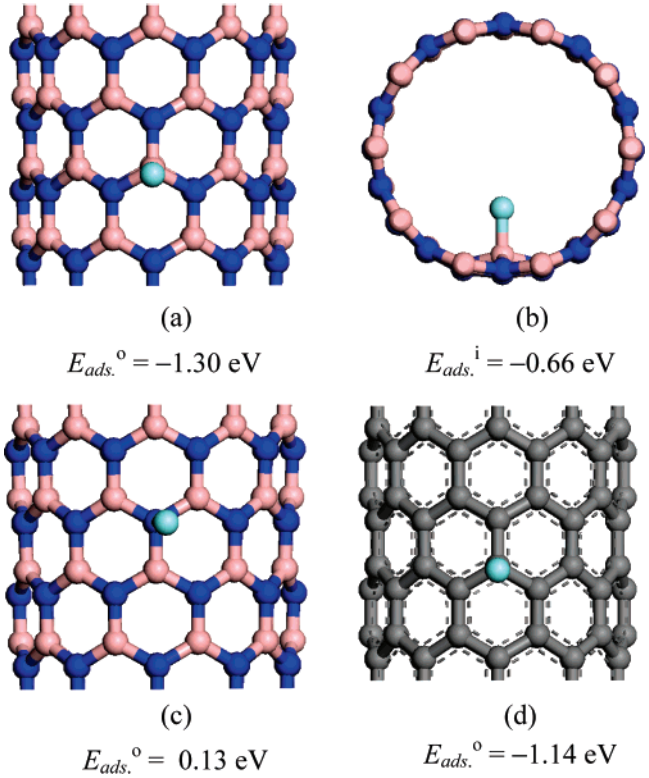

Figure 2. Optimized structures and the associated energies (per F adsorption) for F adsorption in (10,0) BN and C nanotubes. "i" and "o" denote that F atom is adsorbed inside and outside the tube walls, respectively. B, N, C, and F atoms are denoted using orange, blue, gray, and light blue balls, respectively.

3. Results and Discussion

3.1. Fluorine Chemisorption on (10,0) BN SWNTs. An F atom can be chemisorbed on BN nanotube sidewalls. We have considered both endohedral and exohedral adsorption and all the possible unique sites for F chemisorption on (10,0) BN SWNTs, including at B and N atoms, in the center of the six-membered ring (6MR), and at the bridge sites of B−N bonds. However, only three sites (Figure 2a−c) are energetically stable as local minima. The other possible adsorption sites are unstable, and the F's move to more favorable locations upon optimization with geometric relaxation. Exohedral binding at boron (adsorption energy of −1.30 eV, Figure 2a) is the most favorable energetically among the three local minima structures (Figure 2a−c), followed by endohedral fluorine chemisorption at boron (adsorption energy −0.66 eV, Figure 2b). The positive adsorption energy (0.13 eV, Figure 2c) of the exohedral fluorine chemisorption at nitrogen indicates that F is not bound to N energetically when based on F_2 as the reactant. The best configuration, with F attached to an exohedral B atom, is similar to the adsorption of H in BN nanotubes,[20] and agrees with previous theoretical results.[11] The binding energy for the most favorable fluorine chemisorption (−1.30 eV, Figure 2a) on (10,0) BNNT is slightly higher than that of F attached to (10,0) carbon SWNT (Figure 2d) (adsorption energy −1.14 eV, close to previous theoretical results at PBE/6-31G* and B3LYP/6-31G*//PBE/6-31G* level,[21] if (as in this study) we use the energy of a single F atom for adsorption energy evaluation.

As is typical for chemical functionalization of carbon nanotubes,[22,23] fluorine addition to carbon nanotubes forms new C−F bonds, the carbon changes from sp^2 to sp^3 hybridization, and local structural deformation occurs. Similarly, F chemisorption in BNNTs also switches the tube surface atom bound to F from sp^2 to sp^3 hybridization, and induces a local structural

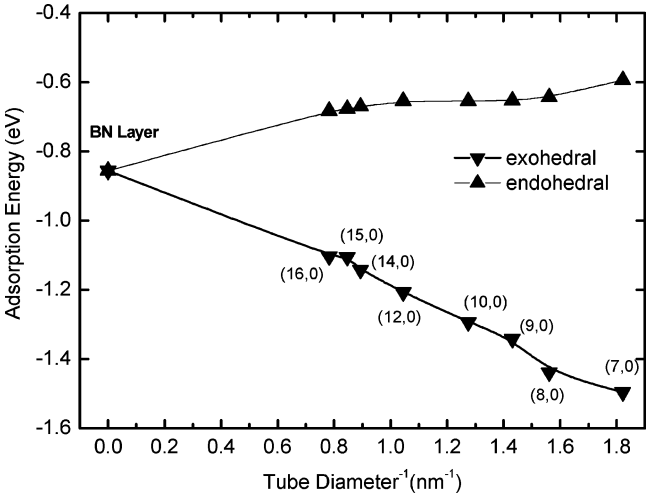

Figure 3. Exohedral (▼) and endohedral (▲) chemisorption energies (per F adsorption) of F above B atom in BN graphitic sheet and SWNTs as function of the inverse of tube diameters (*D*). The two lines are given to show the trend clearly.

deformation. In the lowest-energy configuration (Figure 2a, exohedral binding over a B atom), the B−N bond lengths and angles involving the F-adsorbed B atom (1.53 Å, 1.55 Å, 1.55 Å, 110.4°, 110.5°, and 107.6°, respectively) are close to those in the sp^3-hybridized cubic BN phase (1.567 Å and 109.5°, respectively),[24] but differ from those in the perfect BN nanotube with sp^2 hybridization (1.44−1.45 Å and 116.3−119.9°, respectively). For the second-lowest-energy configuration (Figure 2b, endohedral binding over a B atom), F-induced rehybridization from sp^2 to sp^3 is less pronounced (the bond lengths involving the F-adsorbed B atom are all 1.52 Å, while the bond angles are 113.8°, 113.7°, and 115.4°, respectively). For the third-lowest-energy configuration (Figure 2c, exohedral binding to N), the chemisorption of F only induces slight modification of the local structure of the host BN nanotube (the bond lengths involving the F-adsorbed N atom are all 1.46 Å, while the bond angles are 120.2°, 118.3°, and 119.7°, respectively). The newly formed B−F bond in the more stable exohedral adduct (1.42 Å, Figure 2a) is also shorter than that in the endohedral isomer (1.51 Å, Figure 2b).

3.2. Fluorine Chemisorption on BN Graphitic Sheet and BN SWNTs with Various Diameters. Chemisorption energies for F binding to the optimal B sites for a BN graphitic sheet and BN SWNTs with various diameters (both exohedral and endohedral adsorption) are shown in Figure 3. Because of the curvature effect,[23,25] exohedral adsorption is more favorable than endohedral, especially in the smaller diameter BNNTs. Thus, F atoms prefer to be bound to the convex surface. The magnitude of the exohedral B−F binding energies decreases sharply, whereas the magnitude of the endohedral binding energies increases gradually with increasing BN tube diameter. Hence, the energies of endohedral and exohedral adsorption get closer in larger nanotubes, and approach the limit of the planar BN graphene layer. The highest binding energy is −1.50 eV, when F is attached to B atom outside the (7,0) BN nanotube of 0.55 nm in diameter. On the other hand, F chemisorption on a BN graphitic sheet still possesses a rather high adsorption energy, i.e., −0.85 eV at a B atom.

Linear fitting of exohedral adsorption energy to the inverse of the tube diameter in Figure 3 yields a coefficient of 0.36 eV/nm. A recent DFT calculation gives fitting coefficients of 0.86 and 0.64 eV/nm for F chemisorption on metallic and semiconducting carbon SWNTs, respectively.[23a] The smaller diameter-dependent coefficient for F chemisorption energy on BN tube might be due to its larger band gap, since F chemisorption energy on metallic carbon nanotubes shows more pronounced diameter dependence than that on the semiconducting tubes.

3.3. Chemisorption of Two F Atoms on (10,0) BN SWNTs. Two F atoms on C and BN nanotubes were simulated with a three-unit supercell model. The stable configurations are presented in Figure 4.

Two F atoms are adsorbed on (10,0) C nanotubes most favorably at two adjacent C atoms (Figure 4a); the adsorption energy is about −1.54 eV per F atom.

However, two chemisorbed F atoms in BN nanotubes prefer placements as far away as possible at symmetric sites (Figure 4h). The adsorption energies are as high as −1.26 eV per F atom, and approach that of single F atom chemisorption (−1.30 eV, Figure 2a). The two newly formed B−F bond lengths are 1.42 Å. This lowest-energy structure is followed closely by the configuration with two F atoms adsorbed on two B sites in the same BN hexagon (Figure 4e, adsorption energy −1.23 eV per F atom). The configurations with two F atoms located above two adjacent B and N atoms (Figure 4f) or above two B and N atoms opposite in the same BN hexagon (Figure 4 g) are less stable (adsorption energies −1.14 and −0.88 eV, respectively).

These results are quite different from the adsorption of two F atom in carbon SWNT[12a] or two H atoms in C[26] and BN nanotubes,[20] where external attachment to two adjacent tube surface atoms is preferred. The high stability of the F-absorbed BNNTs presented in Figure 4h may be due to the counteraction of the local structural deformation when the F atoms are far away. Moreover, the adsorption energies of two F atoms on (10,0) BN nanotubes are smaller than those on (10,0) C nanotubes, indicating that BN nanotubes are less prone to fluorination than carbon nanotubes.

3.4. Fluorine Adsorption on BN Double-Walled Nanotubes (DWNTs). Since most BN nanotubes are multiwalled,[27] we simulated the F adsorption in BN (7,0)@(15,0) DWNTs to mimic the F adsorption behavior in BN multiwalled nanotubes (MWNTs). After full structural relaxation the interwall distance is calculated to be about 3.23 Å, comparable to the previously calculated[17] and experimental results.[1a,28]

For isolated (7,0) and (15,0) BN SWNTs, due to the curvature effect,[23,25] F prefers the external attachment to the B site (Figure 5). However, after the (7,0) and (15,0) BN SWNTs are assembled into a DWNT by van der Waals and electrostatic interactions, the favorable F chemisorption site changes completely. When F atom is adsorbed on the top of B inside (7,0) BN tube (Figure 5A) and in the interwall region (Figure 5B,C) of the DWNT, the F chemisorption energies are much lower than those at the same site of isolated BN SWNTs (Figure 5a−c), because of the restriction on the strain energy release of the inner tube wall imposed by the inner−outer tube interaction (for Figure 5A) and the repulsion between the F atom and the BN tube wall (for Figure 5B,C). On the other hand, the binding energy (−1.10 eV) of F adsorption at B in the outer surface of the DWNT, i.e., the outer wall of (15,0) BN tubes (Figure 5D), is very close to the binding energy of an F attached to B atom outside the isolated BN (15,0) tube (−1.11 eV, Figure 5d). Therefore, F chemisorption on BN DWNTs (and even MWNTs) at the B atoms in the outer tube wall is preferred. A very recent experiment found that the fluorine atoms are attached covalently to the outer tube shell of the double-walled carbon nanotubes.[29]

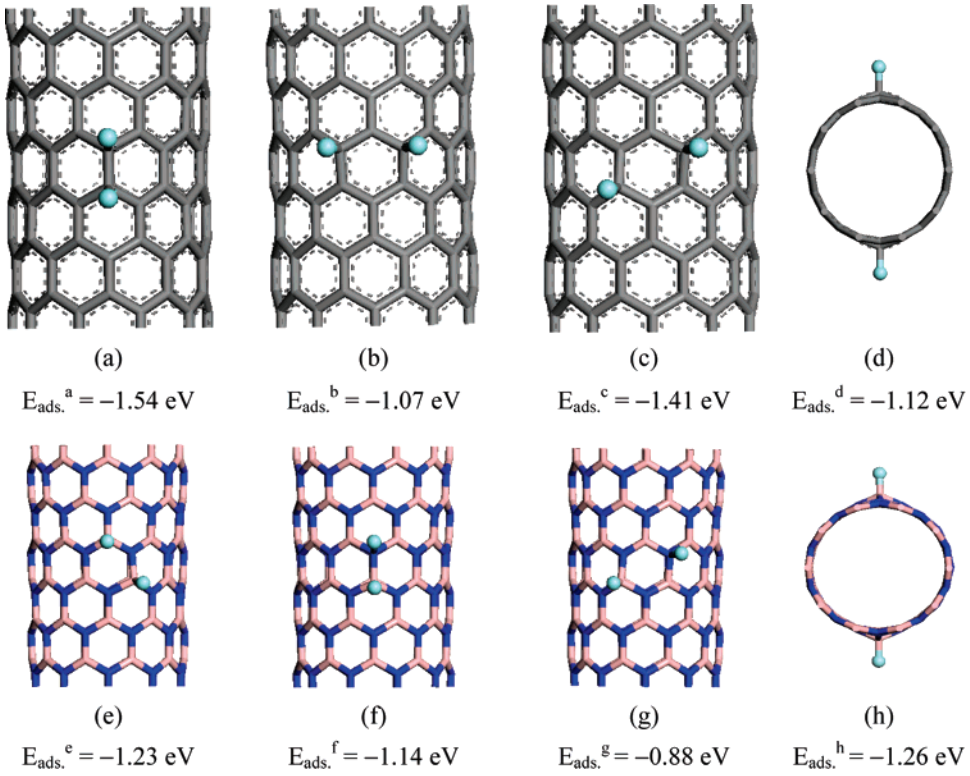

Figure 4. Stable chemisorption states of two F atoms on the wall of (10,0) C and BN SWNTs and related F adsorption energies (per F adsorption). Gray, light blue, dark blue, and pink represent carbon, fluorine, nitrogen, and boron atoms, respectively.

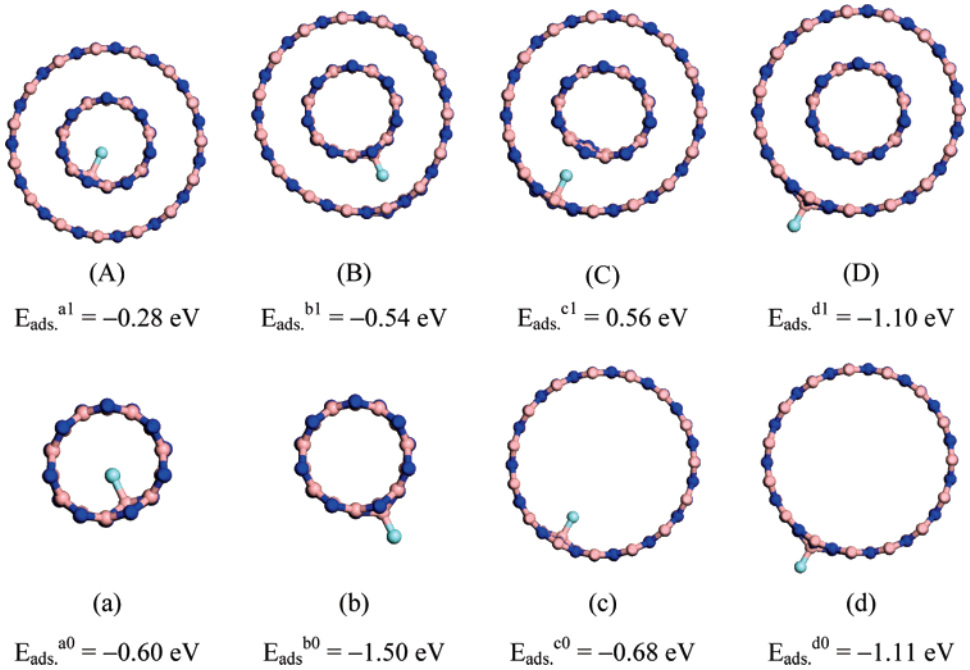

Figure 5. Fluorine chemisorption in (7,0)@(15,0) BN DWNT compared with F chemisorbed in isolated (7,0) and (15,0) BN SWNTs.

3.5. BN (10,0) Nanotubes with Different F Coverages. The fluorine coverage can be controlled by varying the number of F atoms in supercells comprised of one, two, or three unit cells. Lower F coverages of 1.25%−25% correspond to 2−30 F atoms in the two- or three-unit supercells (with 40 B atoms and 40 N atoms or 60 B atom and 60 N atoms in the tube, respectively), while the higher 50% F coverage corresponds to 20 F atoms added to the PBC supercells with only one unit cell (with 20 B atom and 20 N atoms in the tube). In all cases, the F atoms are chemisorbed on BN tubes symmetrically. For a given F coverage, a number of possible configurations were tested, and the adsorption energies are listed in Figures 6−8 for comparison. The most stable isomers were used to calculate the band structures.

As with two F atoms absorbed in (10,0) BN nanotubes (Figure 4), four F atoms (3.33% F coverage, Figure 6) also prefer to bind to B atoms and at symmetric sites separated as much as possible (Figure 6e). The same features results when eight F atoms are included in the supercell with 60 B and 60 N atoms, or when 10 F atoms are included in the supercell with 40 B and 40 N atoms, corresponding to F coverages of 6.67% and 12.5%, respectively.

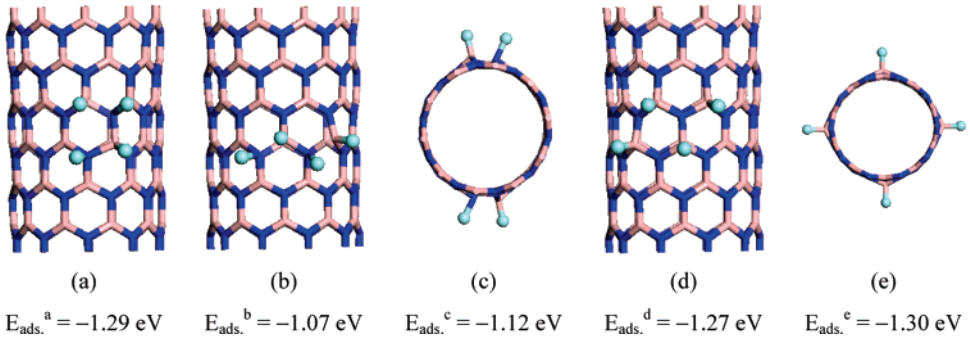

Figure 6. Stable chemisorption states of four F atoms on the wall of (10,0) BN SWNT supercell with 60 B atoms and 60 N atoms (3.33% F coverage) and related F adsorption energies (per F adsorption). Four F atoms are located at (a) a contiguous B−N in the same six-membered ring, (b) a contiguous B−N around a zigzag chain, (c) two B−N units as far away as possible, (d) discrete B atoms as near as possible, and (e) discrete B atoms as far away as possible.

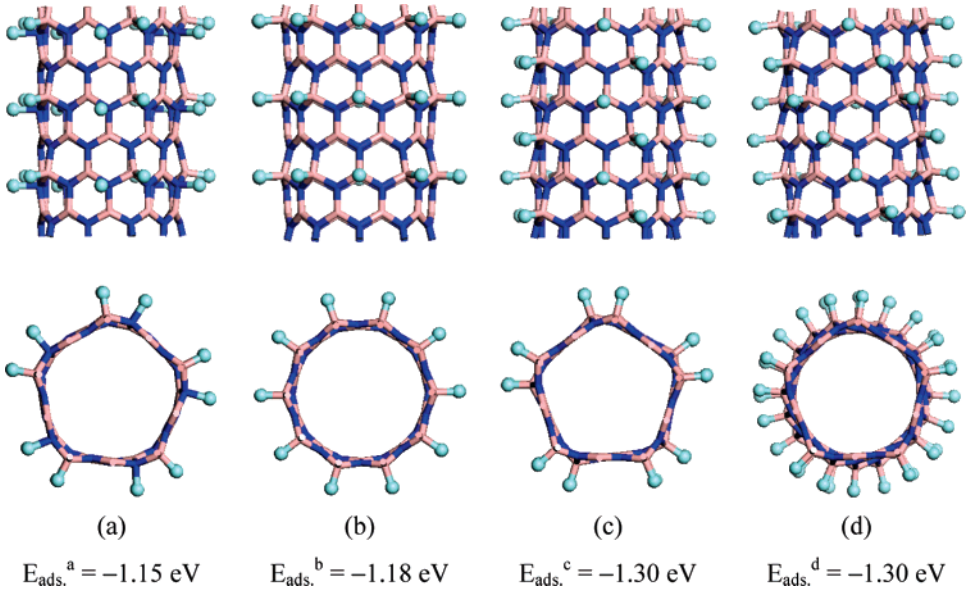

Figure 7. Stable chemisorption states of 30 F atoms on the wall of (10,0) BN SWNT supercell with 60 B atoms and 60 N atoms (25% F coverage) and related F adsorption energies (per F adsorption). The 30 F atoms are located at (a) discontinuous B−N around the tube wall, (b) B atoms around the tube wall, (c) B atoms along the tube axis, and (d) B atoms along the tube wall axis in a helix.

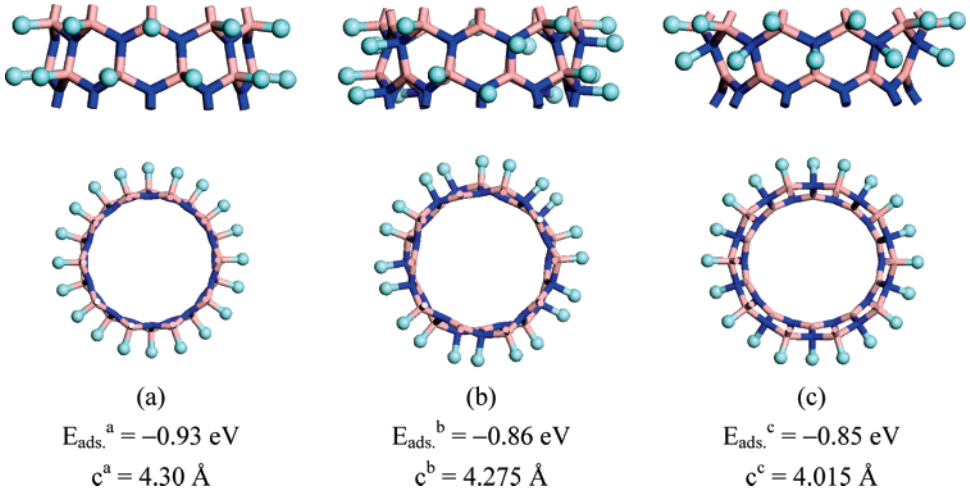

Figure 8. Stable configurations of 20 F atoms on the wall of (10,0) BN SWNT PBC supercell with 20 B atoms and 20 N atoms (50% F coverage) and related F adsorption energies (per F adsorption). The 20 F atom locations are at (a) all B atoms, (b) discontinuous B−N placements around the tube wall, and (c) a continuous B−N ring around the tube wall.

Fluorination coverage of 25% was represented by a supercell with 30 F, 60 B, and 60 N atoms (Figure 7). The F atoms are distributed to B atoms along the tube axis. The 50% F coverage was modeled by a one-unit supercell with 20 F, 20 B, and 20 N atoms, and the unit cell lengths (*c*) were also optimized. The results are listed in Figure 8.

When the F coverage reaches 50%, the F atom binding is still solely to boron (Figure 8a). Since large structural deforma-

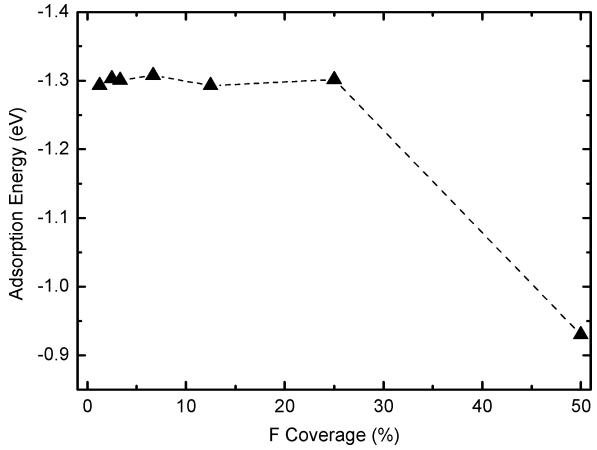

Figure 9. Variation of adsorption energies (per F adsorption) of the most stable configuration with F coverage.

tions are introduced into the tube walls at such a high coverage, the adsorption energy decreases greatly from the rather flat curve for the lower F coverage (Figure 9). The small, but still significant binding energy at 50% F coverage indicates that it is still possible to achieve the same upper limit of fluorination (F/C = 0.5) for BN nanotubes as for their carbon analogues.[12] Full F coverage (100%) requires that all 40 F atoms bind to all 20 B and 20 N atoms in a one-unit supercell exohedrally, or 40 F atom attachments from both exohedral and endohedral directions. However, no stable structures could be obtained after full geometry optimization, since half the F atoms dissociate from the tube wall.

3.6. Changes in Band Structure of BN (10,0) Nanotubes with F Coverage. The electronic band structures were calculated for the most stable BN (10,0) SWNTs with each F coverage. The pristine (10,0) BN nanotube has the typical wide band gap of semiconductors ($E_g \sim 3.96$ eV, Figure 10a), reasonably consistent with previous theoretical results.[2,18,30]

The fluorinated BNNTs at very low F coverage (with one or two F atoms in a two-unit PBC supercell) have been investigated by Yang et al.[9a] for (10,0) BNNT and by Zhang et al.[9b] for (8,0) BNNT. We obtained similar results (shown in Figure 10b,c). At very low F coverage, impurity levels appear above the valence band maxima (VBM), indicating that fluorination results in p-type semiconductors. However, when the F ratio is higher than 12.5%, a great number of empty levels appear above VBM and form a new conduction band, which is separated by a large gap from the original conduction band. Noticeably, the valence band and the newly formed conduction band merge (insets in Figure 10); hence, the highly fluorinated BN nanotubes are converted into p-type conductors. Consequently, the electronic band structures of BN nanotubes can be modified by fluorination.

Tang et al.[10] have reported the only currently available fluorination experiment for BN nanotubes. They synthesized

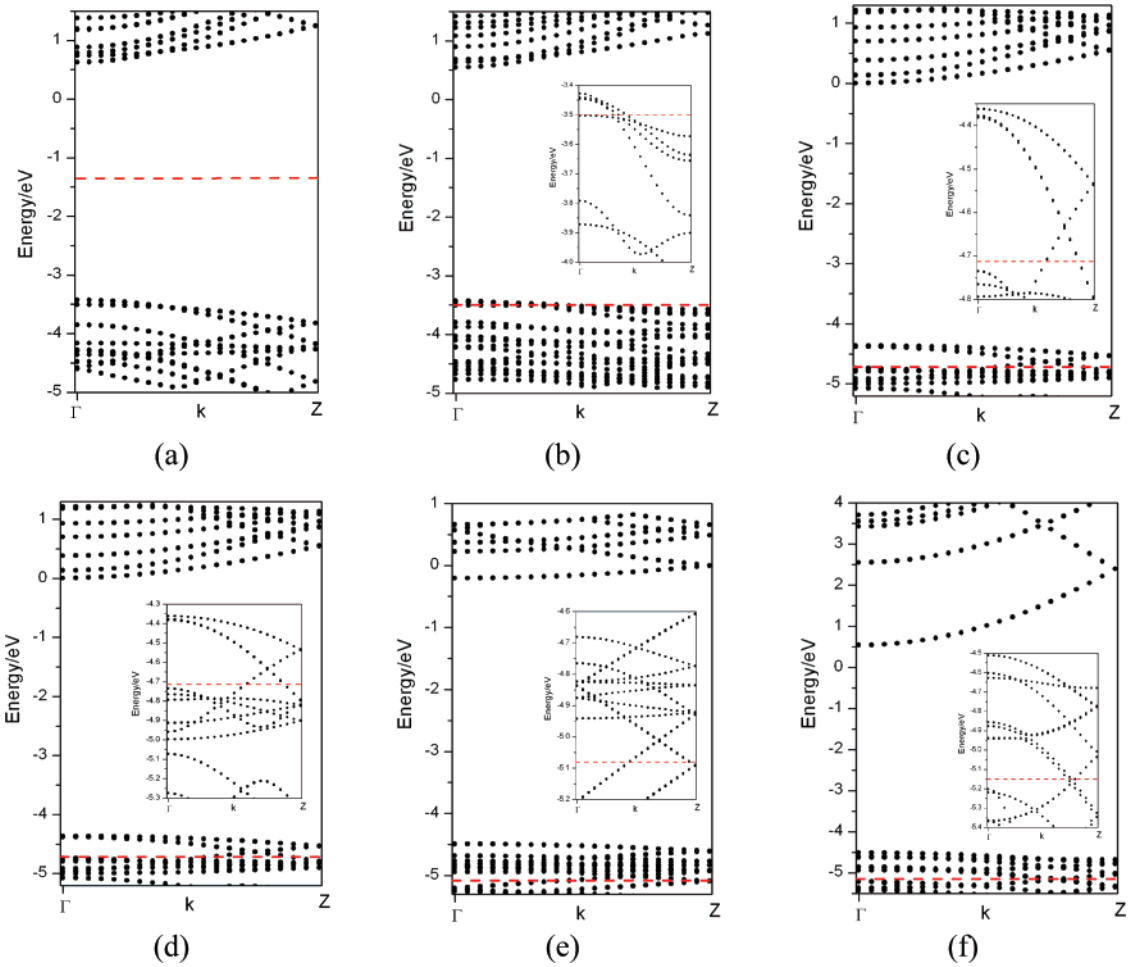

Figure 10. Calculated electronic band structures for BN (10,0) SWNT with (a) 0%, (b) 1.25%, (c) 3.33%, (d) 12.5%, (e) 25%, and (f) 50% F coverage. All band structures are calculated for the most stable configurations of the BN nanotubes with different F coverages. The red broken lines indicate the position of Fermi levels. The inserts in (b)−(f) are enlargements around the Fermi levels.

F-doped (substitution and addition) BN nanotubes by introducing elemental fluorine at the stage of multiwalled nanotube growth. According to our computational results, the reactions between BN nanotubes and F_2 molecules are exothermic. Although more difficult than in C nanotubes, fluorination can occur providing that BN nanotubes are used to react with F_2. It is even possible in fluorinated BNNTs to reach the upper modification limit (F/C = 0.5) for carbon nanotubes.[12] Further studies on the fluorine-functionalized BN nanotubes are needed in order to apply them in nanoelectronics.

3.7. Comparison with NH_3-Modified BNNTs. Very recently, Zeng et al.[31] found that the chemical modification of BN nanotubes (BNNTs) with either NH_3 or amino functional groups results in little change in the electronic structures. This is in stark contrast to the fluorinated BNNTs. Thus, we extended our studies to the NH_3-modified BNNTs following the same computational method as for fluorinated BNNTs, and we investigated the possibility of modifying the band structures of BNNTs by increasing the modification ratio.

At low coverage, NH_3 molecules are chemically bound to BN nanotubes and new B−N bonds form between BN nanotubes and NH_3 molecules (binding energies are −0.16 and −0.14 eV, the B−N bond lengths are 1.75 and 1.77 Å, respectively, at 1.25% and 2.5% NH_3 coverage). However, these chemical bonds are much weaker than those of F−B bonds in fluorinated BN nanotubes. When the coverage reaches 12.5%, NH_3 molecules are only physically adsorbed on BN nanotubes with weak interaction (−0.01 eV) and far distance (∼2.7 Å), indicating a typical von der Waals interaction (see Supporting Information).

There is no significant change in the band structures of BNNTs at different NH_3 modification ratios (see Supporting Information). The wide-band-semiconductor character of BN nanotubes remains regardless of the NH_3 adsorption concentration.

4. Conclusion

The chemisorption of fluorine in BN single-walled nanotubes was investigated by density functional theory (DFT) calculations. At low F coverages (below 50%), F atoms prefer to be attached at the B positions as far apart as possible, and the adsorption energies at different F coverages are quite close. At 50% coverage, F atoms still prefer to be located above the B atoms; the adsorption energy decreases sharply but remains exothermic. Hence, a very high fluorination ratio (50%) can occur when pristine BN nanotubes react with F_2. Such preferable fluorination patterns and highly exothermic reaction energies also hold true for double-walled (and multiwalled) BNNTs when the outer surface is considered. Fluorination affects the electronic properties of BNNTs. Some empty levels appear above the valence band maxima (VBM) at low F coverages, transforming BNNTs into p-type semiconductors; however, fluorinated BNNTs are p-type conductors at high modification ratios. Accordingly, fluorination can "tune" the band structures of BN nanotubes. Further experimental and theoretical investigations on fluorine-functionalized BN nanotubes are needed to realize their possible applications in nanoelectronics.

Note Added in Proof. After the acceptance of this manuscript, Zhi et al.[32] published their theoretical studies on engineering electronic structure of boron-nitride nanotubes by covalent functionalization.

Acknowledgment. This study was supported in China by NSFC (50502021) and in U.S.A. by NSF Grant CHE-0209857. Z.Z. acknowledges the NKU Startup Funding and Dr. Tianying Yan for technical support in the use of the NKStar supercomputer and VASP.

Supporting Information Available: Optimized geometries and computed electronic band structures of BN nanotubes with different NH_3 modification ratios. This material is available free of charge via the Internet at http://pubs.acs.org.

References and Notes

(1) (a) Chropra, N. G.; Luyken, R. J.; Cherrey, K.; Crespi, V. H.; Cohen, M. L.; Louie, S. G.; Zettl, A. *Science* **1995**, *269*, 966. (b) Bengu, E.; Marks, L. D. *Phys. Rev. Lett.* **2001**, *86*, 2385. (c) Loiseau, A.; Willaime, F.; Demoncy, N.; Hug, G.; Pascard, H. *Phys. Rev. Lett.* **1996**, *76*, 4737. (d) Menon, M.; Srivastava, D. *Chem. Phys. Lett.* **1999**, *307*, 407. (f) Deepak, F. L.; Vinod, C. P.; Mukhopadhyay, K.; Govindaraj, A.; Rao, C. N. R. *Chem. Phys. Lett.* **2002**, *353*, 345. (g) Lee, R. S.; Gavillet, J.; de la Chapelle, M. L.; Loiseau, A.; Cochon, J. L.; Pigache, D.; Thibault, J.; Willaime, F. *Phys. Rev. B* **2001**, *64*, 121405.

(2) Rubio, A.; Corkill, J. L.; Cohen, M. L. *Phys. Rev. B* **1994**, *49*, 5081.

(3) Crespi, V. H.; Cohen, M. L.; Rubio, A. *Phys. Rev. Lett.* **1997**, *79*, 2093.

(4) (a) Yoshioka, T.; Suzura, H.; Ando, T. *J. Phys. Soc. Jpn.* **2003**, *72*, 2656. (b) Miyamoto, Y.; Rubio, A.; Cohen, M. L.; Louie, S. G. *Phys. Rev. B* **1994**, *50*, 4976. (c) Blase, X.; Charlier, J. C.; De, Vita, A.; Car, R. *Appl. Phys. Lett.* **1997**, *70*, 197.

(5) (a) Schmidt, T. M.; Baierle, R. J.; Piquini, P.; Fazzio, A. *Phys. Rev. B* **2003**, *67*, 113407. (b) Piquini, P.; Baierle, R. J.; Schmidt, T. M.; Fazzio, A. *Nanotechnology* **2005**, *16*, 827.

(6) (a) Xiang, H. J.; Yang, J. L.; Hou, J. G.; Zhu, Q. S. *New J. Phys.* **2005**, *7*, 39. (b) Mickelson, W.; Aloni, S.; Han, W. Q.; Cumings, J.; Zettl, A. *Science* **2003**, *300*, 467.

(7) Han, W. Q.; Zettl, A. *J. Am. Chem. Soc.* **2003**, *125*, 2062.

(8) Li, J.; Zhou, G.; Liu, H.; Duan, W. *Chem. Phys. Lett.* **2006**, *426*, 148.

(9) Wu, X.; Zeng, X. C. *J. Chem. Phys.* **2006**, *125*, 044711.

(10) Tang, C.C.; Bando, Y.; Huang, Y.; Yue, S.L.; Gu, C.Z.; Xu, F.F.; Golberg, D. *J. Am. Chem. Soc.* **2005**, *127* (18), 6552.

(11) (a) Xiang, H. J.; Yang, J.; Hou, J. G.; Zhu, Q. *Appl. Phys. Lett.* **2005**, *87*, 243113. (b) Lai, L.; Song, W.; Lu, J.; Gao, Z.; Nagase, S.; Ni, M.; Mei, W. N.; Liu, J.; Yu, D.; Ye, H. *J. Phys. Chem. B* **2006**, *110*, 14092. (c) Zhang, J.; Loh, K. P.; Yang, S. W.; Wu, P. *Appl. Phys. Lett.* **2005**, *87*, 243105. (d) Zhang, J.; Loh, K. P.; Deng, M.; Sullivian, M. B.; Zheng, J.; Wu, P. *J. Appl. Phys.* **2006**, *99*, 104309.

(12) See reviews: (a) Bettinger, H. F. *ChemPhysChem* **2003**, *4*, 1283. (b) Khabashesku, V. N.; Billups, W. E.; Margrave, J. L. *Acc. Chem. Res.* **2002**, *35*, 1087. (c). Lu, X.; Chen. Z. *Chem. Rev.* **2005**, *105*, 3643.

(13) Mickelson, E. T.; Chiang, I. W.; Zimmerman, J. L.; Boul, P. J.; Lozano, J.; Liu, J.; Smalley, R. E.; Hauge, R. H.; Margrave, J. L. *J. Phys. Chem. B* **1999**, *103*, 4318.

(14) Kudin, K. N.; Bettinger, H. F.; Scuseria, G. E. *Phys. Rev. B* **2001**, *63*, 45413.

(15) Solubilized with amino functional groups, BN nanotubes can be dissolved in water, and polymer wrapped BN nanotubes are soluble in various organic solvents. See: (a) Xie, S. Y.; Wang, W.; Fernando, K. A. S.; Wang, X. Lin, Y.; Sun, Y. P. *Chem. Commun.* **2005**, 3670. (b) Zhi, C.; Bando, Y.; Tang, C.; Xie, R.; Sekiguchi, T.; Golberg, D. *J. Am. Chem. Soc.* **2005**, *127*, 15996.

(16) (a) Wang, Y.; Perdew, J. P. *Phys. Rev. B* **1991**, *44*, 13298. (b) Kresse, G.; Hafner, J. *J. Phys.: Condens. Matter* **1994**, *6*, 8245. (c) Kresse, G.; Hafner, J. *Phys. Rev. B* **1994**, *49*, 14251.

(17) Perdew, J. P.; Wang, Y. *Phys. Rev. B* **1992**, *45*, 13244.

(18) (a) Golberg, D.; Bando, Y. *Appl. Phys. Lett.* **2001**, *79*, 415. (b) Ma, R.; Bando, Y.; Sato, T.; Kurashima, K. *Chem. Mater.* **2001**, *13*, 2965. (c) Lee, R. S.; Gavillet, J.; Chapelle, M. Lamy de la; Loiseau, A.; Cochon, J. L.; Pigache, D.; Thibault, J.; Willaime, F. *Phys. Rev. B* **2001**, *64*, 121405.

(19) (a) Okada, S.; Saito, S.; Oshiyama, A. *Phys. Rev. B* **2002**, *65*, 165410. (b) Okada, S.; Saito, S.; Oshiyama, A. *Physica B* **2002**, *323*, 224.

(20) (a) Xiang, H. J.; Yang, J. L.; Hou, J. G.; Zhu, Q. S. *Phys. Rev. B* **2003**, *68*, 035427. (b) Wu, X. J.; Yang, J. L.; Hou, J. G.; Zhu, Q. S. *J. Chem. Phys.* **2004**, *121*, 8481. (c) Zhou, Z.; Zhao, J.J.; Chen, Z.F.; Gao, X.P.; Yan, T. Y.; Schleyer, P. V. *J. Phys. Chem. B.* **2006**, *110*, 13363.

(21) Bettinger, H. F.; Kudin, K. N.; Scuseria, G. E. *J. Am. Chem. Soc.* **2001**, *123*, 12849.

(22) Zhao, J. J.; Chen, Z. F.; Zhou, Z.; Park, H.; Schleyer, P. V.; Lu, J. P. *ChemPhysChem* **2005**, *6*, 598.
(23) (a) Park, H.; Zhao, J. J.; Lu, J. P. *Nanotechnology* **2005**, *16*, 635. (b) Zhao, J. J.; Park, H. K.; Han, J.; Lu, J. P. *J. Phys. Chem. B* **2004**, *108*, 4227.
(24) Christensen, N. E.; Gorczyca, I. *Phys. Rev. B* **1994**, *50*, 4397.
(25) (a) Chen, Z. F.; Thiel, W.; Hirsch, A. *ChemPhysChem* **2003**, *4*, 93. (b) Lu, X.; Tian, F.; Xu, X.; Wang, N.; Zhang, Q. *J. Am. Chem. Soc.* **2003**, *125*, 10459.
(26) Han, S. S.; Lee, H. M. *Carbon* **2004**, *42*, 2169.
(27) Golberg, D.; Bando, Y.; Kurashima, K.; Sato, T. *Solid State Commun.* **2000**, *116*, 1.
(28) Chen, X.; Gao, X. P.; Zhang, H.; Zhou, Z.; Hu, W. K.; Pan, G. L.; Zhu, H. Y.; Yan, T. Y.; Song, D. Y. *J. Phys. Chem. B* **2005**, *109* (23), 11525.
(29) Bulusheva, L. G.; Gevko, P. N.; Okotrub, A. V.; Lavskaya, Yu. V.; Yudanov, N. F.; Yudanova, L. I.; Abrosimov, O. G.; Pazhetnov, E. M.; Boronin, A. I.; Flahaut, E. *Chem. Mater.* **2006**, *18*, 4967.
(30) Zhou, Z.; Zhao, J. J.; Chen, Z. F.; Gao, X. P.; Lu, J. P.; Schleyer, P. v. R.; Yang, C.-K. *J. Phys. Chem. B* **2006**, 110, 2529.
(31) Wu, X. J.; An, W.; Zeng, X. C. *J. Am. Chem. Soc.* **2006**, *128*, 12001.
(32) Zhi, C.; Bando, Y.; Tang, C.; Golberg, D. *Phys. Rev. B* **2006**, *74*, 153413.